IOP Conf. Series: Materials Science and Engineering **779** (2020) 012055 doi:10.1088/1757-899X/779/1/012055

Development and research of a borehole centrifugal pump stage

V Cheremushkin[1,3], V Lomakin[1], N Kalin[1] and A Trulev[2]

[1]Bauman Moscow State Technical University
[2]AO «Rimera»

[3]E-mail:vcheremushkin@bmstu.ru

Abstract. This article is devoted to the model of a borehole centrifugal pump developed at the Department of Hydraulics of Bauman Moscow State Technical University. A universal layout has been developed for testing the stages of pumps of this type in a certain range of parameters. The article describes the mathematical model used. A comparison of numerical and field experiments is given. A problem has been identified when comparing their results.

1 Introduction

Currently, there is a huge scope of borehole pumps. For example, in the oil industry, in the agricultural, in everyday life. There are a lot of variations of such pumps and each one needs its own approach for testing.

The main number of such pumps are used in everyday life, for pumping water from wells. To date, no work has been done on the numerical study of this type of pump with small dimensions.

This work is associated with developments underway at the Department of Hydraulics of Bauman Moscow State Technical University. On the basis of the Department, a variant of the borehole centrifugal pump stage was developed. To obtain a wet part suitable for the given parameters, optimization was carried out using numerical hydrodynamic modeling.

Currently, two main areas of optimization of borehole centrifugal pumps are CFD modeling and improvement of gas-liquid centrifugal separators [1]. There is also a way to improve energy efficiency by improving control algorithms [2].

To conduct full-scale tests of the developed pump, a universal prototype was designed and produced, on which various flow parts can be tested with a fairly wide range of parameters and sizes. Figure 1 shows the design of such a layout.

The design includes universal units for supplying and discharging liquids, which also contain bearings and mechanical seals. The shaft has a margin in length, and the spacers in the form of a honed pipe between the elbows are interchangeable. Thus, the design of the layout allows one to test the stages of different radial and axial dimensions. Limitations in radial dimensions are 100 mm in diameter, since the inner diameter of the honed pipe is 100 mm. The axial limitation is only the length of this pipe and the length of the shaft. If necessary, the shaft can be made in a different length.

3D models of the impeller and the guide vanes were created (Figure 2), and subsequently made using 3D printing. The material is polyamide.

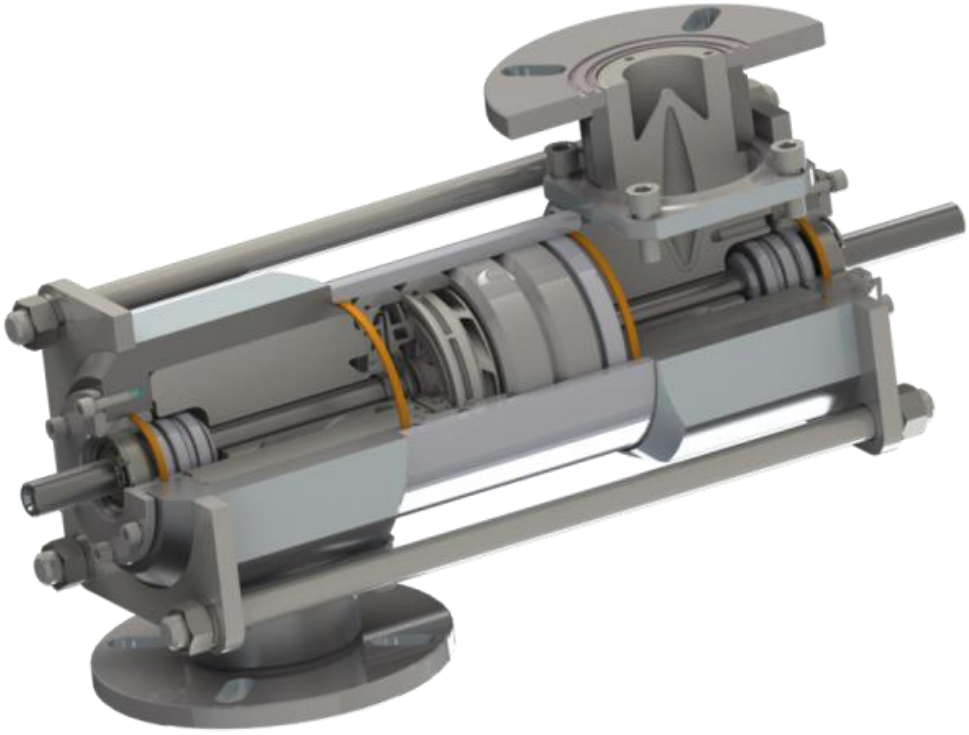

Figure 1. Stages test layout

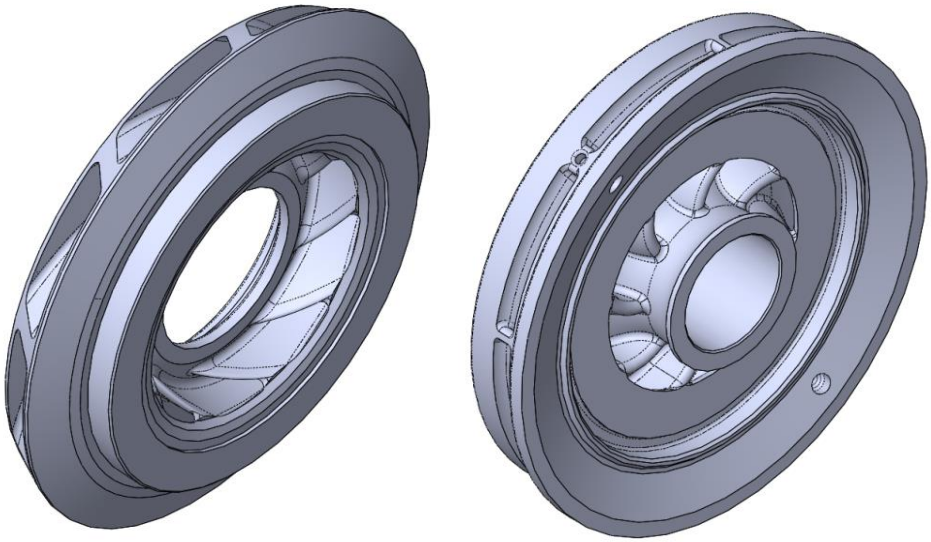

Figure 2.3D models of the impeller and guide vanes

The impeller is equipped with a bronze bushing (Figure 3) for precise alignment along the shaft, and the guide vanes is equipped with a metal sleeve (Figure 4) for centering in a honed tube.

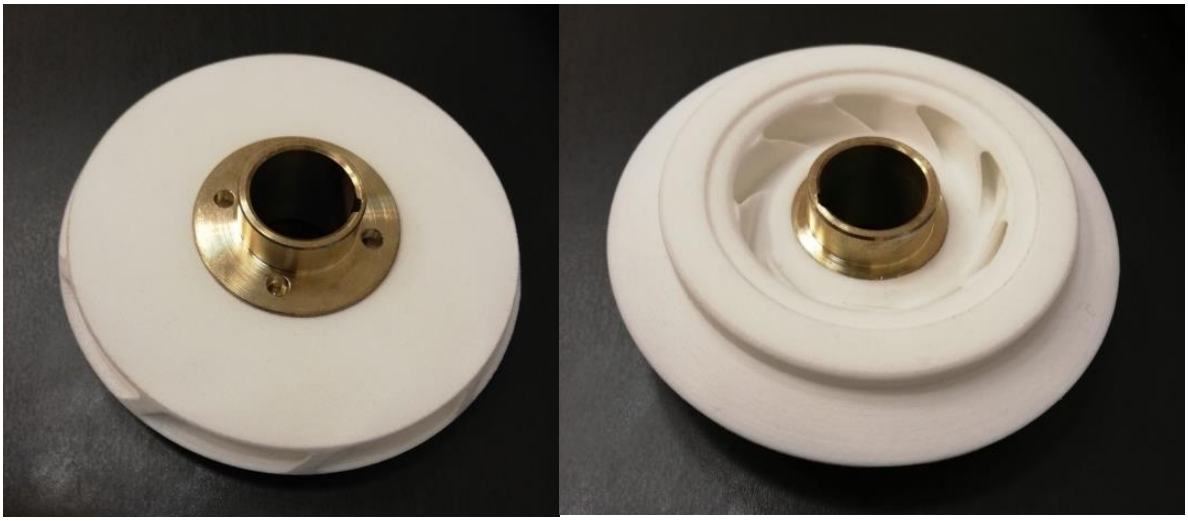

Figure 3. Printed impeller with glued bronze bushing

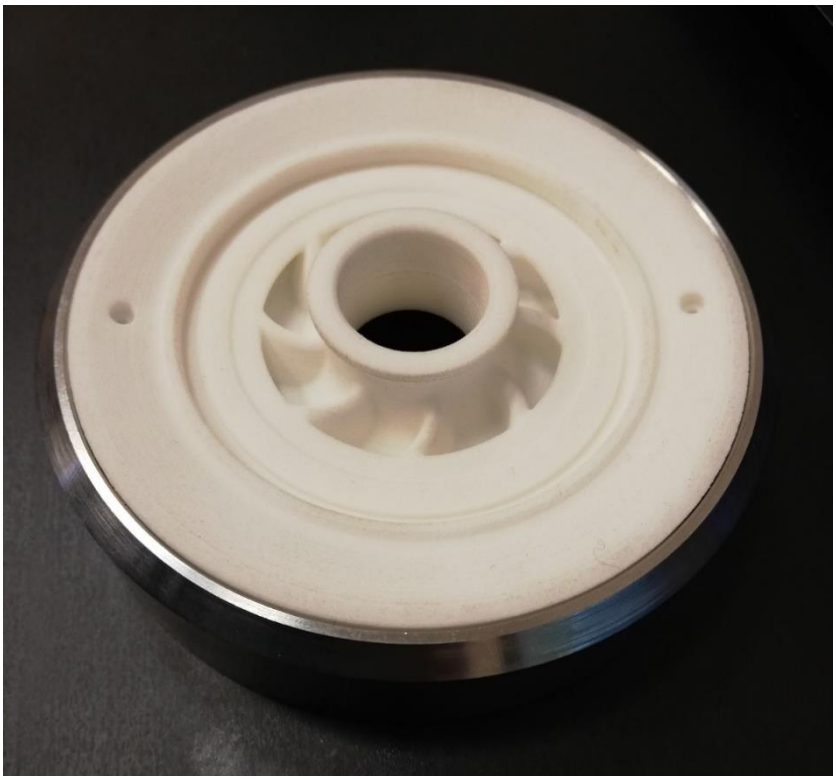

Figure 4. Printed guide vanes glued to a metal sleeve

2 Problem statement and mathematical model.

The task was to develop stages for a borehole pump with certain parameters at a shaft speed of 2910 rpm.

To obtain a stage suitable for these parameters, the method of numerical hydrodynamic modeling was used to calculate the flow in the impeller and guide vanes.

The method of numerical simulation is based on the solution of discrete analogues of the basic equations of hydrodynamics [3, 4, 5]. In the case of an incompressible fluid model (ρ=const), this is:

Mass conservation equation (continuity equation)

$$\frac{\partial \tilde{u}_j}{\partial x_j} = 0,$$

where $\tilde{u}_j$ is the averaged value of the fluid velocity in the projection onto the jth axis (j=1,2,3);

Momentum conservation equation (averaged by Reynolds):

$$\rho\left[\frac{\partial U_i}{\partial t} + U_j \frac{\partial U_i}{\partial x_j}\right] = -\frac{\partial P}{\partial x_i} + \frac{\partial}{\partial x_i}\left[T_{ij}^{(v)} - \rho\langle u_i u_j\rangle\right];$$

where U, P — averaged speed and pressure;

$\tilde{T}_{ij}^{(v)} = 2\mu\tilde{s}_{ij}$ —viscous stress tensor for an incompressible fluid;

$\tilde{s}_{ij} = \frac{1}{2}\left[\frac{\partial \tilde{u}_i}{\partial x_j} + \frac{\partial \tilde{u}_j}{\partial x_i}\right]$ is the instantaneous strain rate tensor;

$\rho\langle u_i u_j\rangle$ — Reynolds stresses.

The introduction of the Navier-Stokes equations averaged by Reynolds makes the system of equations not closed, as additional unknowns appear - Reynolds stresses. To close the system, the semi-empirical k-ω SST turbulence model is used, which introduces the necessary additional equations: the equations of transfer of turbulence kinetic energy and the relative dissipation rate of this energy [6, 7, 8, 9]:

$$\frac{\partial k}{\partial t} + U_j \frac{\partial k}{\partial x_j} = P_k - \beta^* k\omega + \frac{\partial}{\partial x_j}\left[\left(\nu + \sigma_k \nu_T\right)\cdot\frac{\partial k}{\partial x_j}\right]$$

$$\frac{\partial \omega}{\partial t} + U_j \frac{\partial \omega}{\partial x_j} = \alpha\cdot S^2 - \beta\cdot\omega^2 + \frac{\partial}{\partial x_j}\left[\left(\nu + \sigma_\omega \nu_T\right)\cdot\frac{\partial \omega}{\partial x_j}\right] + 2\cdot\left(1-F_1\right)\cdot\sigma_{\omega 2}\cdot\frac{1}{\omega}\cdot\frac{\partial k}{\partial x_i}\cdot\frac{\partial \omega}{\partial x_i}$$

The roughness function f is used to take into account the wall roughness:

$$f = \begin{cases} 1 & если\ R^+ < R^+_{smooth} \\ \left[B\cdot\left(\frac{R^+ - R^+_{smooth}}{R^+_{rough} - R^+_{smooth}}\right)\right]^a & если\ R^+_{smooth} < R^+ < R^+_{rough}; \\ B + CR^+ & если\ R^+ > R^+_{rough} \end{cases}$$

$$R^+ = \frac{ru^*}{\nu}, \text{где}$$

r— equivalent roughness value,

ν – kinematic viscosity,

u^*—characteristic velocity near the wall, determined depending on the turbulence model used.

$$a = sin\left[\frac{\pi}{2}\frac{\log\left(R^+ / R^+_{smooth}\right)}{\log\left(R^+_{rough} / R^+_{smooth}\right)}\right];$$

R^+_{smooth} —roughness value corresponding to smooth walls;

R^{+}_{rough} – R + value for roughness corresponding to a rough wall.

Then the logarithmic velocity profile is determined according to the expression:

$$u^{+} = \frac{1}{K} ln\left(\frac{E}{f} y^{+}\right), \text{where}$$

$$y^{+} = \frac{yu^{*}}{\nu};$$

y— distance from the wall;

K and E— constants.

The wet part of the borehole pump stage was modeled on a grid consisting of 739 thousand cells. In the core of the flow stream, the cells have a multifaceted shape; at the solid walls of the pipe, they are prismatic [10, 11]. The calculation grid for the stage is shown in the Figure 5.

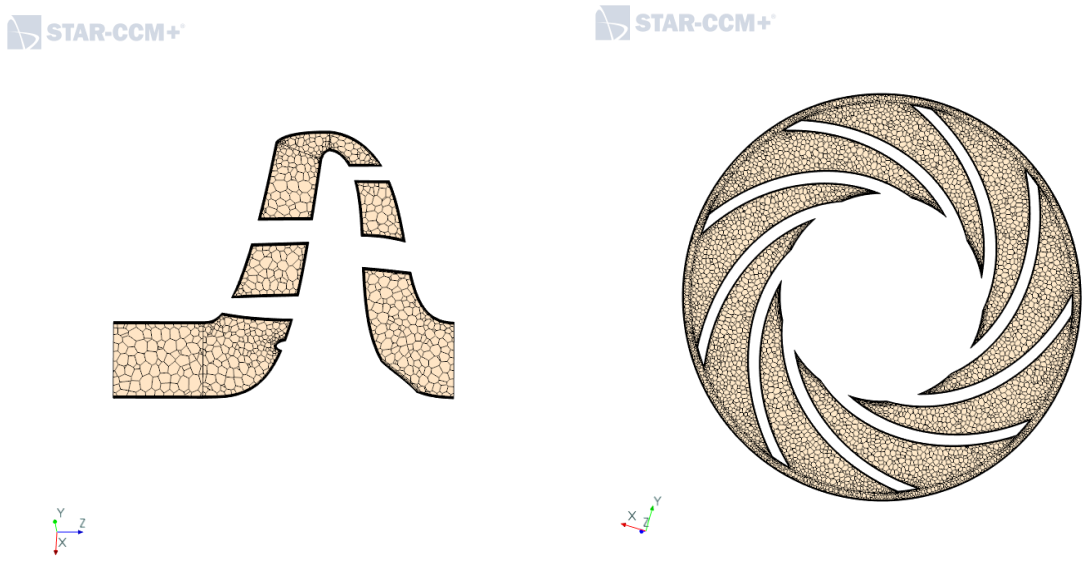

Figure 5. Calculation grid

3 Optimization results

To obtain the best characteristics, suitable for the given requirements, 512 different models of the wet part of the stage were selected. Variable parameters and the range of their changes are presented in table 1.

Table1. Variableparameters

Variableparameter	Parameterchangerange
Outletbladeangle,β_2, °	20-35
Wrap angle of impeller blade, φ, °	90-130
Wrap angle of guide vanes channel, φ_s°	80-110
Impeller outlet width,b_2, mm	5-6

The optimization results are presented in table 2.

Table2. Optimization results

Model no.	Q/Qnom	H/Hnom	Efficiency, %
0	1	1.11	68.49
1	1	1.08	68.48
2	1	1.15	68.01
3	1	1.09	68.92
4	1	1.12	65.84
5	1	1.12	68.24
…	…	…	…
112	1	1.12	68.41
…	…	…	…
507	1	1.11	68.63
508	1	1.06	65.75
509	1	1.10	67.90
510	1	1.09	68.14
511	1	1.10	66.73
512	1	0	0

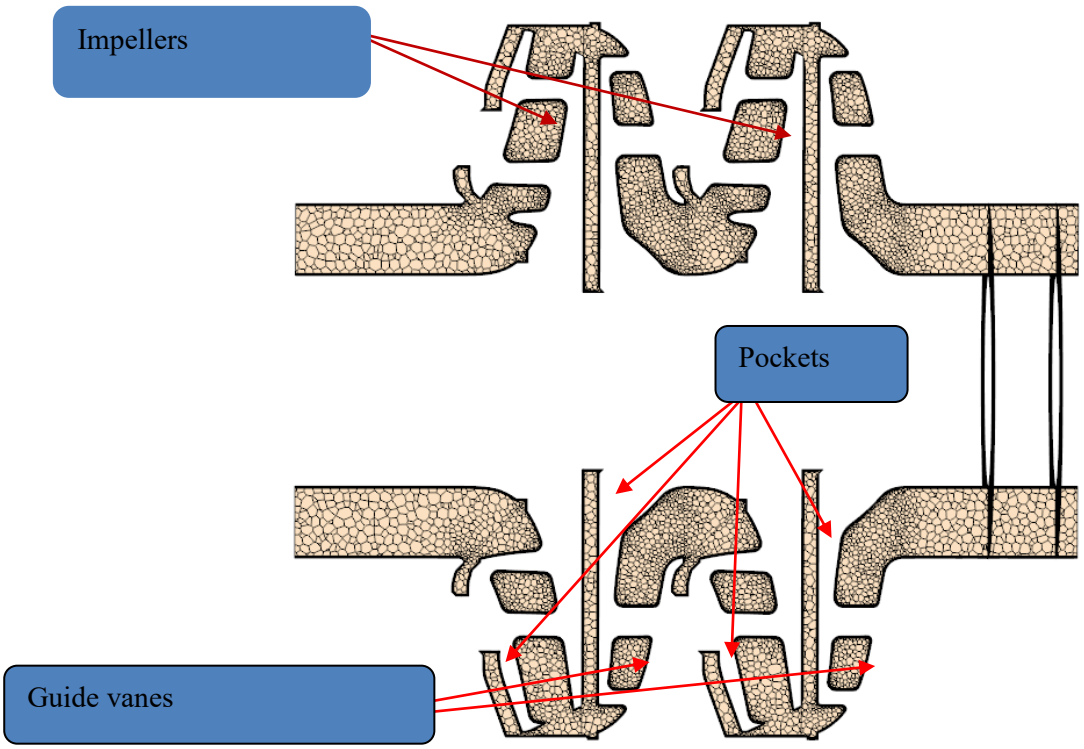

Figure 6. Calculation grid

The best model is No. 112. For it, a hydrodynamic numerical calculation was made in the unsteady mode of two stages, taking into account the pockets. In this calculation, the roughness of the walls, the mathematical model of which is described above, was taken into account. The calculation grid of the wet part is shown in the figure 6. It consists of 3290000 cells

The figure below shows scenes of the distribution of reference values in cross sections, such as velocities, pressures, and turbulent kinetic energy.

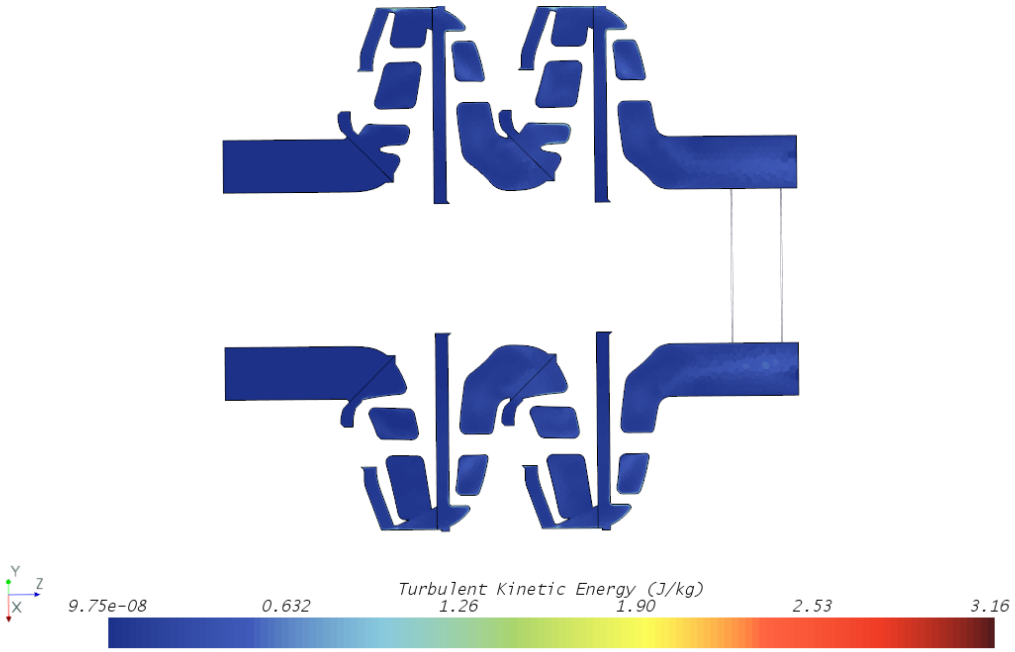

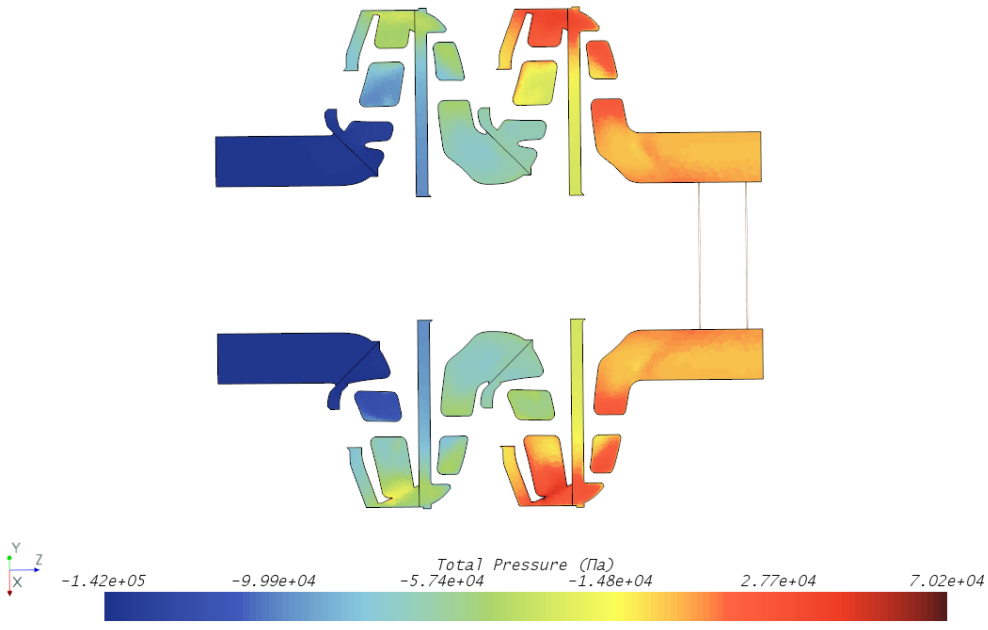

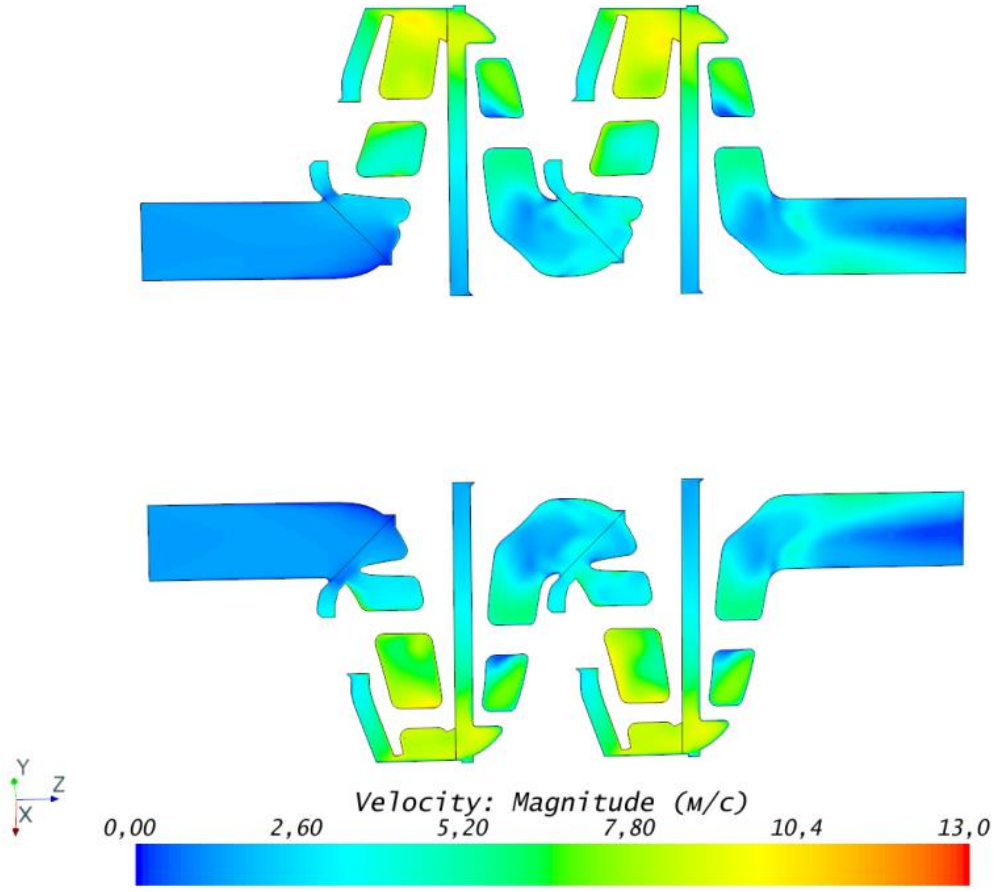

Figure 7. Scalar distribution scenes

The table shows the main parameters of the resulting optimized wet part after modeling of two stages, taking into account the roughness of the walls and the flow of fluid particles in the pockets.

Table 3

Model no.	Q/Qnom	H/Hnom	Efficiency,%
112	1	0.96	59.3

4 Field tests on the developed layout

To determine the hydraulic characteristics of the profiled wet part, its bench tests were carried out on a universal prototype (according to GOST 16504-81). The figure shows the layout mounted on the stand, as well as a general view of the test bench.

Tests were conducted for two and four stages. The resulting graphs are presented in figures 9 and 10.

Efficiency is given minus the dry friction moment — 0.45 N*m

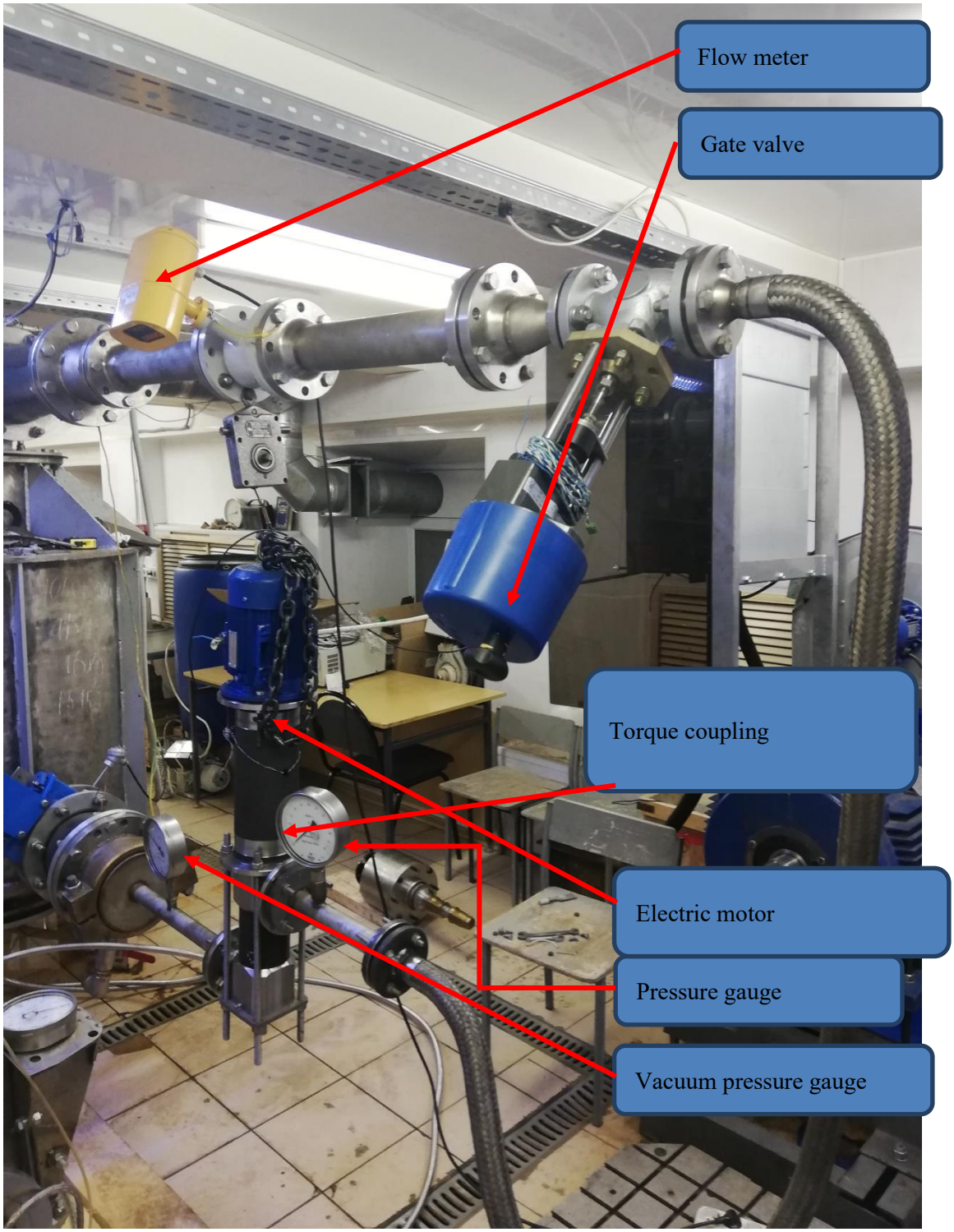

Figure 8. Test bench

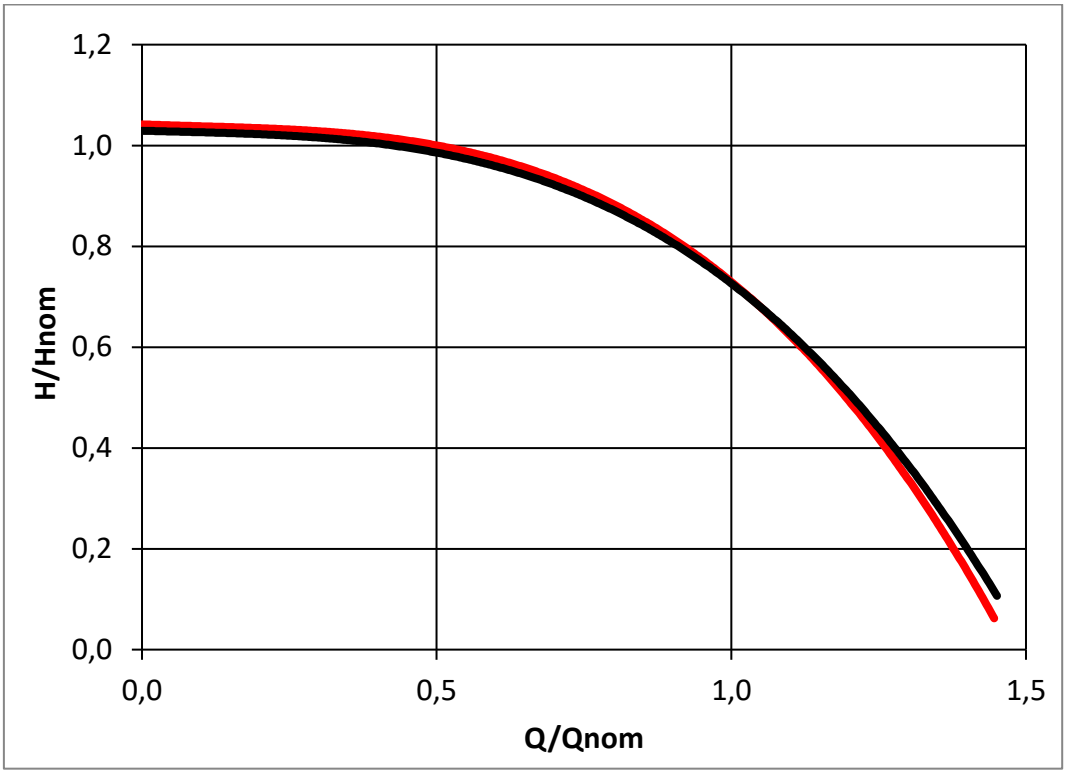

Figure 9. Pressure characteristics for 2 and 4 stages, rated to nominal

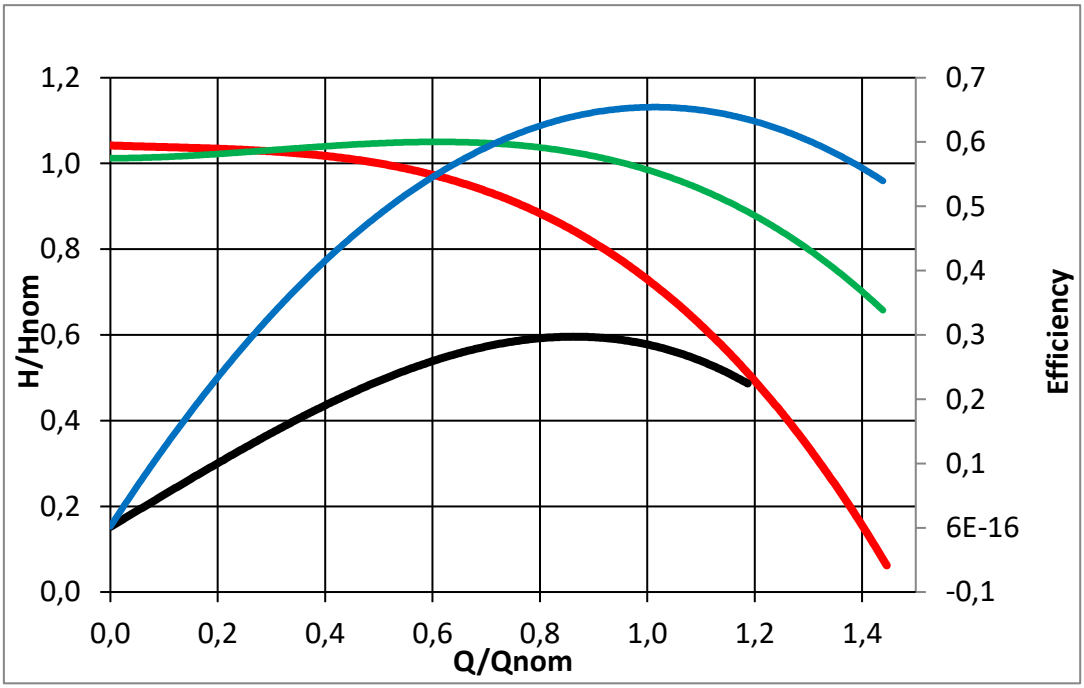

Figure 10. Pressure characteristics and efficiency obtained during field tests and by the method of hydrodynamic modeling. The black graph is the efficiency of the full-scale mock-up, the blue graph is the efficiency obtained using CFD modeling. The red characteristic is the pressure of the full-scale mock-up, the green characteristic is the pressure obtained using CFD modeling.

Table 4 compares the results of numerical calculation and experiment.

Table 4. Comparison of experimental and calculated data

Data	Head, m	Efficiency, %
Experiment	21,1	28,6
Calculation, 1 stage (conversion to 4 stages)	30,4	64,9
Calculation, 2 stages (conversion to 4 stages)	30,2	64,8
Calculation, 2 stages, taking into account the roughness (conversion to 4 stages)	28,4	59,5

5 Conclusion on the work performed

As a result of the work done by means of numerical hydrodynamic modeling, the wet part of the borehole centrifugal pump stage was obtained, which corresponds to the given parameters. To verify the conformity of the results of numerical calculation and field testing, a universal layout was designed. As a result, the efficiency obtained in the calculation numerically and in full-scale test differs by almost 2 times. A significant difference in pressure was also obtained, which can be seen in the comparative characteristics. The assumption was made that the error arose due to the fact that the roughness was not taken into account in the simulation. This assumption was verified by adding a roughness to the mathematical function, which affects the velocity distribution near solid walls. However, even taking into account the roughness, no correspondence was obtained between the numerical and field tests. Further research in this area is necessary to explain the results.

References.

[1] Budaev, G, Danilov, D, Kuznechov, A, Lomakin, V, Cheremushkin, V. Research of centrifugal gas-liquid separator // IOP Conference Series: Materials Science and Engineering, Vol.589 (1), № 012035. DOI: 10.1088/1757-899X/589/1/012035

[2] Brunman, V.E., Vataev, A.S., Volkov, A.N., Larin, M.Y., Matsko, O.N., Petkova, A.P., Plotnikov, D.G. Improving the energy efficiency of borehole pumps.(2017) Russian Engineering Research, 37 (7), pp. 579–580. DOI: 10.3103/S1068798X17070061

[3] Cheremushkin, V., Polyakov, A. Optimization of the output device of a disk pump for high viscous fluid // IOP Conference Series: Materials Science and Engineering, Vol.589 (1), № 012001. DOI: 10.1088/1757-899X/589/1/012001

[4] Lomakin, V.O., Chaburko, P.S., Kuleshova, M.S. Multi-criteria Optimization of the Flow of a Cen-trifugal Pump on Energy and Vibroacoustic Characteristics // Procedia Engineering. Vol. 176, 2017, pp 476–482. DOI: 10.1016/j.proeng 2017.02.347.

[5] Lomakin, V.O. Investigation of two-phase flow in axial-centrifugal impeller by hydrodynamic mod-eling methods. Proceedings of 2015 International Conference on Fluid Power and Mechatronics, FPM 2015, 2015, № 7337302, Pp 1204–1206. DOI: 10.1109/FPM.2015.7337302

[6] Loitsianskii, L.G. Mechanics of liquisd and gases / Loitsianskii, L.G. -Moscow: Drofa, 2003. — 840p.

[7] Gouskov, A.M., Sorokin, F.D., Banin, E.P. Simulation of an Inlet Structure of an Implantable Axial Blood Pump. Biomedical Engineering, Vol 50, 2016, Pp 15-19. DOI: 10.1007/s10527-016-9578-2 13. Gouskov, A.M., Lomakin, V.O., Banin, E.P., Kuleshova, M.S. Minimization of Hemolysis and Im-provement of the Hydrodynamic Efficiency of a Circulatory Support

Pump by Optimizing the Pump Flowpath. Biomedical Engineering, Vol 51, 2017, Pp 229–233. DOI: 10.1007/s10527-017-9720-9

[8] Baturin, O., Popov, G., Kolmakova, D., Zubanov, V., Novikova, J., Korneeva, A. Optimization of Powerful Two-stage Screw Centrifugal Pump. 2nd International Conference on Mechanical, System and Control Engineering, ICMSC 2018; Moscow; Vol 220, 2018. DOI: 10.1051/matecconf/201822003009

[9] Tesch, K.Email Author, Kaczorowska-Ditrich, K. Discrete-continuous optimisation of an axial flow blood pump. 23rd Fluid Mechanics Conference, FMC 2018; Zawiercie; Poland. Vol 1101, 2018. DOI: 10.1088/1742-6596/1101/1/012044

[10] Boyarshinova, A., Lomakin, V., Petrov, A. Comparison of various simulation methods of a two-phase flow in a multiphase pump (2019).IOP Conference Series: Materials Science and Engineering, 589 (1), № 012014. DOI: 10.1088/1757-899X/589/1/012014

[11] Śmierciew, K.Email Author, Gagan, J., Butrymowicz, D. Application of numerical modelling for de-sign and improvement of performance of gas ejector. Applied Thermal Engineering. 2019, Pp 85-93. DOI: 10.1016/j.applthermaleng.2018.12.030